Journal of Applied Polymer Science

Nano-SiO_2-reinforced ultraviolet-curing materials for three-dimensional printing

Congchao Zhang, Yihua Cui, Juan Li, Dandan Jiang
Department of Materials Science and Engineering, College of Materials Science and Technology, Nanjing University of Aeronautics and Astronautics, 29 Yudao Street, Nanjing 210016, People's Republic of China
Correspondence to: Y. Cui (E-mail: cuiyh@nuaa.edu.cn)

ABSTRACT: As an additive manufacturing technology, ultraviolet (UV)-curing three-dimensional printing, which requires the use of a photocurable resin, is increasingly being used to produce customized end-user parts of many complex shapes. In this study, to improve the strength and ductility of printing materials, nano-SiO_2-reinforced photocurable resins were prepared by a planetary ball mill; then, the morphology, photochemistry, thermal property, and mechanical properties of the nanocomposites were investigated and characterized. Transmission electron microscopy analysis indicated that the modified nano-SiO_2 was well dispersed in the photocurable resin. The glass-transition temperature increased from 67.2°C for the unfilled resin to 71.7 and 80.1°C for nanocomposites with nano-SiO_2 contents of 0.3 and 0.7 wt %, respectively. The tensile strength and impact strength were increased by 46.7 and 165.3% for nanocomposites with 0.3 wt % nano-SiO_2. The flexural modulus of the nanocomposites increased from 1.7 to 8.0 GPa when 0.7 wt % nano-SiO_2 was added to the photocurable resin; this appeared to originate from the relatively high level of dispersion and the intimate combination of the nano-SiO_2 with the matrix. The investigation of the physical and chemical properties of such UV-curing materials showed that the low filler concentration (<1 wt %) of nano-SiO_2 did not affect the processability of the nanocomposites. © 2015 Wiley Periodicals, Inc. J. Appl. Polym. Sci. **2015**, *132*, 42307.

KEYWORDS: manufacturing; mechanical properties; photopolymerization

Received 15 January 2015; accepted 6 April 2015
DOI: 10.1002/app.42307

INTRODUCTION

Three-dimensional printing (3DP), also known as *additive manufacturing,* is not just a singular new technology.[1–3] Where the printing press facilitated the diffusion of new ideas, 3DP combines the Internet's fast access to information with what economists calls the Third Industrial Revolution.[4,5] Ultraviolet (UV)-curing 3DP is based on the process of photopolymerization, in which a resin, initially in liquid form, is converted to a solid polymer on exposure to UV laser radiation. The component is produced by the spraying of liquid UV-curing materials layer by layer until a three-dimensional object is formed from nozzle jets not too unlike those in an inkjet printer, as shown in Figure 1.[6] On completion, the three-dimensional component is usually postcured under high-intensity UV light in a UV chamber to complete the polymerization process.[7]

The important mechanical properties of rapid prototyping parts are strength and ductility.[8,9] The poor strength of the rapid prototypes created by 3DP has always been a major problem hindering their application under loading conditions.[10,11] The weak mechanical properties associated with the photopolymer cause the prototype to fracture and lose useable value.[12] During the last few years, an overwhelming amount of researches have been carried out to understand and improve both the process and the photopolymer.[13,14] All of these have been carried out with an aim of achieving prototypes with higher strengths.

Kumar *et al.*[15] studied the mechanical properties of optically curable stereolithographic resins (SLRs); these were reinforced through the addition of small amounts (<5 wt %) of cellulose nanocrystals. A remarkable modulus enhancement was observed. At the same time, the mechanical properties of the SLRs were significantly increased by addition of minute amounts of cellulose nanocrystals.

Cadek *et al.*[16] studied the effect of the interfacial surface area on the tensile behavior of poly(vinyl alcohol) films loaded with different types of carbon nanotubes. Their results indicate that the total nanotube surface area was directly proportional to the tensile reinforcement. They concluded that reinforcement was significantly dependent on the interfacial interactions between the polymer the carbon nanotubes.

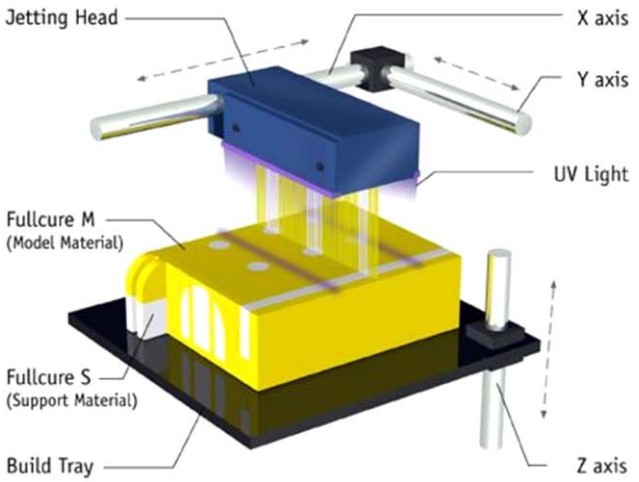

Figure 1. Schematic representation of the UV-curing 3DP process. [Color figure can be viewed in the online issue, which is available at wileyonlinelibrary.com.]

Research on acrylic nanocomposites containing up to 30 wt % silica nanoparticles was developed by Gurr *et al.*[17] for applications in structural light modulation and stereolithography technologies. The results show that the uniform dispersion of nanoparticles afforded significantly improved toughness and stiffness in the photopolymerized and postcured nanocomposites. However, silica nanoparticle concentrations up to 30 wt % gave abundantly higher viscosities.

Improved mechanical properties have been reached with different pathways,[18–20] but in most cases, positive results were accompanied by various difficulties. For example, the length of cellulose nanocrystals and carbon nanotubes is a tremendous challenge, so they are unsuitable for this process because the diameter of the nozzle is about 20 μm.

To solve the problems mentioned previously, In this article, we present and described the results of an experimental study undertaken to investigate the effects of the addition of nano-SiO_2 on the mechanical properties of photocurable resins. To maintain good processability, the viscosity of the UV-curing 3DP formulations had to be kept low so that the content of the filler could be kept as low as possible. During the process of photocuring, the double bonds of the monomer and oligomer were cleaved. Then, polymerization occurred as did double bonds on the other end of 3-(trimethoxysilyl) propyl methacrylate (KH570). Thus, the nano-SiO_2 particles could be firmly embedded in the cured resin. We, therefore, explored in a systematic study how the introduction of small amounts of modified nano-SiO_2 affected the mechanical properties of the UV-curing nanocomposites.

EXPERIMENTAL

Materials

The isopropyl alcohol, oxalic acid, and absolute ethanol used were provided by Nanjing Chemical Reagent Co., Ltd., which were all analytical reagents. KH570 was used to improve the compatibility between the organic polymer and inorganic materials, which was supplied by Nanjing Kemai Chemicals Co., Ltd. Nano-SiO_2 with the average diameter of 20 nm was purchased from Nanjing Xianfeng Nanomaterials Technology Co., Ltd.

The photocurable resin used in this research was a mixture of the acrylate-functionalized oligomers of Guangdong Tianyi HS9103 and Sartomer CN2302, the reactive diluents of Taiwan Changxing 1,6-hexanediol diacrylate and trimethylolpropane trimethacrylate, the reactive amine synergist 6420 supplied by the same company, and the photoinitiator Tianjin Jiuri 369 and isopropyl thioanthone (ITX).

Modification of Nano-SiO_2

The pH value of the mixture of deionized water and ethanol with a volume ratio of 1 : 3, was kept at 4; this was adjusted by the content of oxalic acid. KH570, which was 5% of nano-SiO_2, was dropped into 40 mL of the mixture in drops and hydrolyzed under violent stirring at 25°C for 4 h. Finally, a certain amount of original nano-SiO_2 was taken after drying for 24 h at 80°C, and the mixture was put into a three-necked flask. The reaction was kept at 75°C for 8 h, and then, the modified nano-SiO_2 was obtained.

Composite Fabrication

The reactive diluents 1,6-hexanediol diacrylate, trimethylolpropane trimethacrylate, and photoinitiator 369 and ITX were charged into a beaker, and the mixture was stirred at the speed of 25 rpm for 2 h. Then, a mixture of HS9103 and CN2302 with a mass ratio of 3 : 1 was added to the a beaker. The mixture was vigorously stirred by a magnetic stirring apparatus until it became transparent. The exact dosage for the mixture is listed in Table I; it had a viscosity of 80.5 cps at 25°C. The number-average molecular weight was defined as the molecular weight.

A homogeneous dispersion of nano-SiO_2 in UV-curing resins is a critical aspect of making nanocomposites; it is usually achieved via a three-roll mill or ultrasonication techniques.[21,22] In this research, KH570-modified nano-SiO_2 was dispersed in 50 mL of isopropyl alcohol by the use of an ultrasonic bath for 1 h. Then, the mixture was added to the unfilled resin by a planetary ball mill at a speed of 250 rpm for 9 h. Next, the mixture was ultrasonicated for 15 min to remove the air bubbles; then, the mixture was kept in an oven at 80°C until the isopropyl alcohol was removed completely. Finally, mixture samples with various amounts of nano-SiO_2 from 0.1 to 0.7 wt % were applied onto a polished glass substrate and cured by a UV lamp with a power of 2000 W and an emission wavelength of 365 nm for 40 s layer by layer. Each layer thickness was controlled by a bar coater to be 0.1 mm.

Characterization

Fourier transform infrared (FTIR) spectroscopy spectra of the original and KH570-modified nano-SiO_2 were obtained between 4000 and 400 cm^{-1} with a NEXUS670 FTIR spectrometer from Nicolet. Samples were ground into fine powders and doped with KBr.

The dispersion state of the nano-SiO_2 in the nanocomposites was morphologically characterized by transmission electron microscopy (TEM) images. The nanocomposite specimens were milled into a nanometer powder of about 100 nm, and the

Table I. Composition of the Unfilled Resin

Component	wt %	Description	Functionality	Number-average molecular weight
HS9103	48	Epoxy acrylate	2	5000
CN2302	16	Hyperbranched poly(ester acrylate)	16	375
HDDA	20	1,6-Hexanediol diacrylate	2	226
TMPTMA	10	Trimethylolpropane trimethacrylate	3	338
369	2	2-Benzyl-2-(dimethylamino)-1-[4-(4-morpholinyl)phenyl]-1-butanone	-	366.5
ITX	2	Isopropyl thioanthone	-	241
6420	2	Reactive amine synergist	3	304

sections were dispersed in ethanol by use of an ultrasonic bath for 10 min. The TEM observations were done with a JEM-2100 Tecnai instrument (JEOL, Japanese) with an accelerating voltage of 30 kV.

Photochemical parameters of the nanocomposites were obtained by the following steps. Glass slides were wetted with the respective resin. Defined areas were cured at different scanning speeds (20–30 m/min). The glass slides were cleared of any remaining resin by rinsing with isopropyl alcohol. The resulting films were UV-postcured for 30 min to ensure mechanical integrity. The film thicknesses were measured with a digital calliper with an accuracy of 0.001 mm. For each resin, three working curves were measured at different positions of the building envelope according to the described routine. For adjustment of the building parameters, the measured curing depths (C_d's) were calculated as the average values for a given resin.

The viscosity of each sample was measured with a rotational viscometer with a conical graduate (NDJ-5S Digital Viscometer, Shanghai Fangrui Co., Ltd., 30–60 rpm, 25.0 ± 0.1°C, sample volume = 100 mL).

Differential scanning calorimetry measurements were performed with a 200F3 differential scanning calorimeter from Netzsch Co. All of the cured samples (ca. 10 mg) were heated up from 20 to 200°C at a heating rate of 10°C/min under an argon atmosphere at an argon flow of 20 mL/min. The glass-transition temperature (T_g) was taken at the inflection point of the specific heat increment at the glass–rubber transition.

Tensile tests were carried out according to ASTM D 638 at 25°C. Five dumbbell-shaped specimens with thicknesses of 4 mm were tested for each category of nanocomposites, and the average value is reported. The performed tests were conducted on a 5-kN CMT5105 electronic universal testing machine at a crosshead speed of 5 mm/min. Flexural texts were carried out on rectangular bars (80 × 10 × 4 mm^3, ASTM D 790) with a CMT5105 electronic universal testing machine at room temperature. The impact resistance of the composites was evaluated on an impact tester machine. According to ASTM D 256, Izod impact tests were performed with an energy level of 0.5 J at room temperature. Five unnotched impact test specimens with dimensions of 80 × 10 × 4 mm^3 were examined for each set of nanocomposites.

The morphology of the impact fracture surfaces and microstructure of the nanocomposites after impact tests were observed by scanning electron microscopy with a JSM-6360LV (JEOL, Japan).

RESULTS AND DISCUSSION

Modification of Nano-SiO_2

The surface characteristics of the original and KH570 modified nano-SiO_2 were analyzed by a NEXUS670 FTIR spectrometer. The modification mechanism of nano-SiO_2 by KH570 is shown in Figure 2. The silane of hydrolyzed KH570 and the generated silanol; then, condensation polymerization occurred, and siloxane was produced. Silane could react with the —OH groups that originally existed on the surface of nano-SiO_2. Thus, the strong combination of covalent bonding between KH570 and nano-SiO_2 was established. Figure 3 shows the FTIR spectra of the original nano-SiO_2, where the stretching vibration absorption peaks of H—O—H, Si—OH, and Si—O bonds appeared at 1631, 962, and 800 cm^{-1}. The obvious peak of Si—O—Si appeared and was enhanced at 1105 cm^{-1}; this was due to the Si—O—Si stretching and proved that the interactions between nano-SiO_2 and KH570 were formed.[23] As shown by curve b in Figure 3, there were three new peaks at 1405, 1455, and 1693 cm^{-1}, which corresponded to the characteristic peaks of

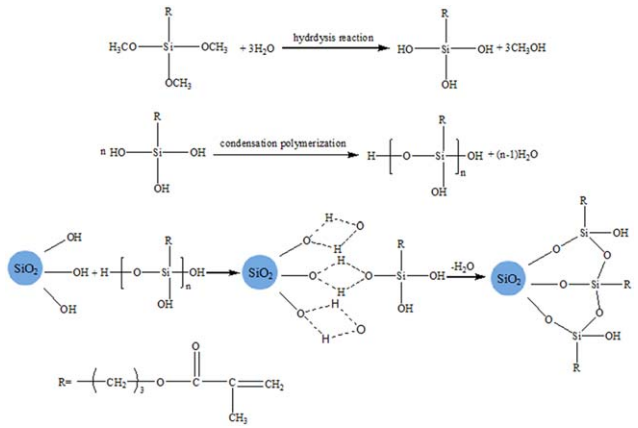

Figure 2. Mechanism of nano-SiO_2 modification. [Color figure can be viewed in the online issue, which is available at wileyonlinelibrary.com.]

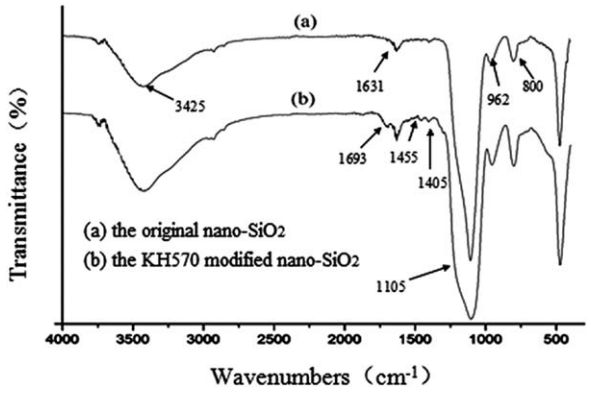

Figure 3. FTIR spectra of different types of nano-SiO_2: (a) original nano-SiO_2 and (b) KH570-modified nano-SiO_2.

C—H coming from —CH_2, —CH_3, and C=C and could only have originated from KH570.[24]

Morphological Characterization

Figure 4 shows the TEM images of nanocomposites contained the original and KH570-modified nano-SiO_2, the nano-SiO_2 content of which was 0.3 wt %. Gratifyingly, the individually separated KH570-modified nano-SiO_2 particles were found in the polymer matrix, whereas the original nano-SiO_2 in the other system aggregated very seriously; this indicated that KH570 modification may have improved the dispersion of nano-SiO_2 in the matrix. As shown in Figure 4(b), several nano-SiO_2 particles, with an average size of about 20 nm, were embedded in the matrix firmly because of the strong interfacial bonding between the nano-SiO_2 and the polymer resin.

Photochemistry and Processing Parameters

The curing exposure (E) was calculated from the intensity measured on the surface of the vat (60 W/m^2) for all of the described experiments and the scanning speed. The relationship between E and C_d, known as the working curve from UV-curing 3DP, was examined for all of the resins.[17] The photochemical parameters followed eq. (1) for a scanning speed up to 30 m/min for all of the resins. Figure 5 shows the working curve of the unfilled resin as an example:

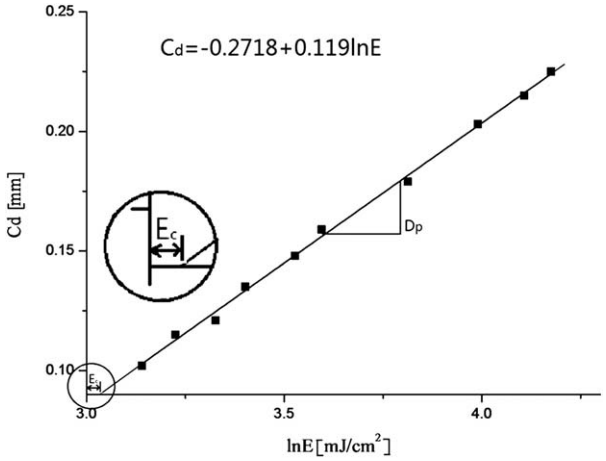

Figure 5. Working curve: C_d versus E for the unfilled resin.

$$C_d = D_p \ln E - D_p \ln E_c \quad (1)$$

The penetration depth (D_p) of the light emitted by the 3DP apparatus into the resin and the critical exposure (E_c) to initiate network formation were evaluated as the slope and exposure intercept, respectively. The layer E for a C_d of 50 μm was determined from each resin's working curve to guarantee a uniform overlap of 10 μm between adjacent layers 30 μm in thickness in the following experiments. The results are summarized in Table II. Increasing filler content led to a slightly decreased C_d for a given E from 0.119 to 0.107 mm for a nano-SiO_2 content of 0.7 wt %. With increasing content of the nano-SiO_2, E_c of the nanocomposites increased from 9.82 mJ/cm^2 to a maximum of 11.64 mJ/cm^2. Both effects corresponded to a decrease in the initiator concentration per volume upon addition of the filler. Contrary effects, such as light scattering or adsorption by filler particles, did not occur or were exceeded by this dilution. To obtain a C_d of 50 μm for all of the resins, values of E, rising from 17.54 mJ/cm^2 for 3DP-1 to 35.58 mJ/cm^2 for 3DP-4, were chosen.

The viscosities of the nonaged resins increased slightly with increasing nano-SiO_2 content; this benefited from the good dispersion of the nano-SiO_2 in the matrix. All of the measured viscosities of the nanocomposites, summarized in Table II, were

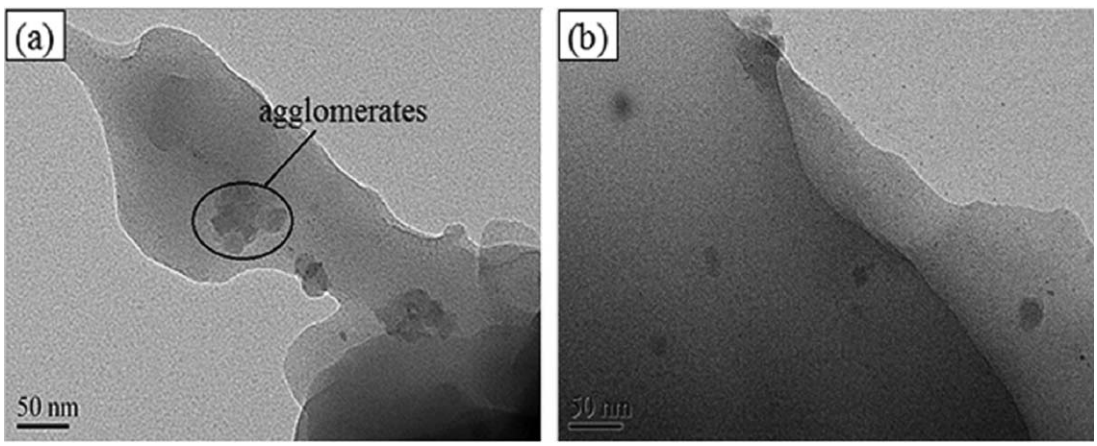

Figure 4. TEM images of the cured nanocomposites with 0.3 wt % filler: (a) original nano-SiO_2 and (b) KH570-modified nano-SiO_2.

Table II. Photochemical Parameters for the Unfilled Resin and Nanocomposites

Resin	Nano-SiO_2 (wt %)	D_p (mm)	E_c (mJ/cm^2)	Viscosity at 25°C (cps)
Unfilled resin	0.0	0.119	9.82	80.5
3DP-1	0.1	0.116	10.31	87.5
3DP-2	0.3	0.112	10.98	88.0
3DP-3	0.5	0.109	11.29	92.0
3DP-4	0.7	0.107	11.64	97.0

below 100 cps; this indicated that this kind of resin could be suitable for UV-curing 3DP processing.

Thermal Properties

The glass transition of polymers is a common phenomenon and emphasizes the necessity of studying T_g. Many dramatic changes in the physical properties take place when it occurs, especially in the mechanical properties.[25,26]

Figure 6 shows that T_g increased with increasing nano-SiO_2 content. When the nano-SiO_2 contents were 0.3 and 0.7 wt %, T_g of the nanocomposites increased from 67.2°C for the unfilled resin to 71.7 and 80.1°C, respectively. This might have benefited from the well-dispersed and stable existing nano-SiO_2 in the system at this content; thus, the system had a relatively high crosslinking degree during the last curing stage. However, the differential scanning calorimetry results did not reflect significant changes in the thermal stability.

Mechanical Properties

Tensile Properties. In the experimental range, the tensile strength of the nanocomposite increased with increasing content of nano-SiO_2, but it acted the opposite when the nano-SiO_2 content was more than 0.5 wt %, as shown in Figure 7. Thus, it offered immediate evidence that the well-dispersed nano-SiO_2 was efficient in transferring the applied load. The results presented in Figure 7 show that the addition of 0.3 wt % nano-SiO_2 to the photocurable resin increased the tensile strength from 21.9 MPa to a maximum of 32.1 MPa. The enhancement

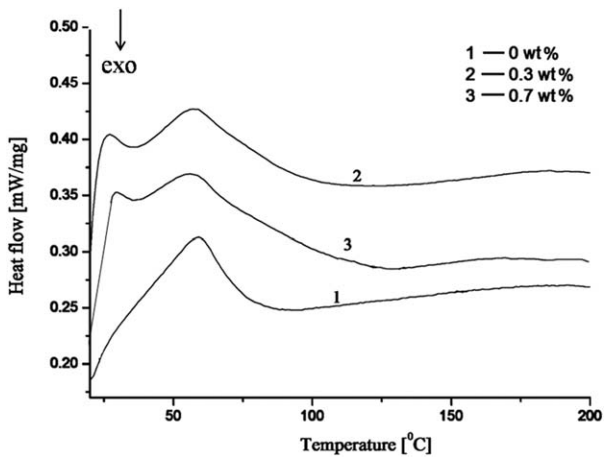

Figure 6. Differential scanning calorimetry curves for different contents of nano-SiO_2.

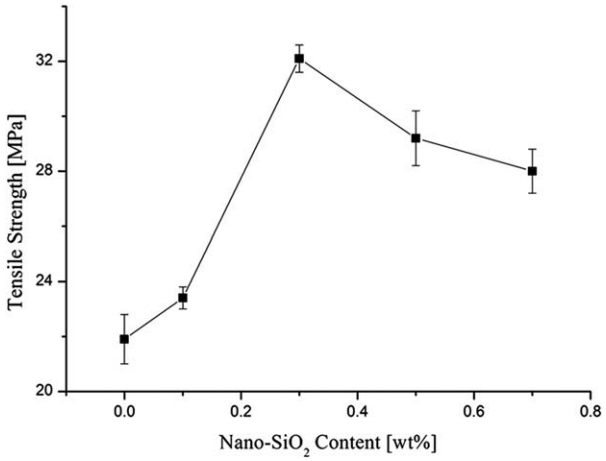

Figure 7. Tensile strength of the nanocomposites as a function of the nano-SiO_2 content.

in the mechanical properties is a general tendency for nanocomposites because the nanomaterials act as reinforcement, and the degree of reinforcement is dependent on the dispersion state of the nanomaterials.[27,28] Although some agglomerates appeared obviously in the matrix as Figure 4(a) shows that when the nano-SiO_2 content was more than 0.3 wt %, they did great harm to the mechanical properties.

The elongation at break is plotted as a function of the nano-SiO_2 content in Figure 8. With increasing nano-SiO_2 content, the elongation at break of the nanocomposites obviously increased. The data showed an enhancement in the elongation at break, where it increased from 7.02 (unfilled resin), 7.11, 7.94, 8.17, and 8.19% for nanocomposites with 0.1, 0.3, 0.5, and 0.7 wt % nano-SiO_2, respectively.

The tensile strength and elongation at break increased from 21.9 MPa and 7.02% to the maximum of 32.1 MPa and 8.19%; these values were not as high as expected. There were two reasons that might explain this results. The first reason was that the bonding between nano-SiO_2 and the surrounding matrix was not strong enough to support a stronger stress. It was reported that the interfacial bonding between the nano-SiO_2

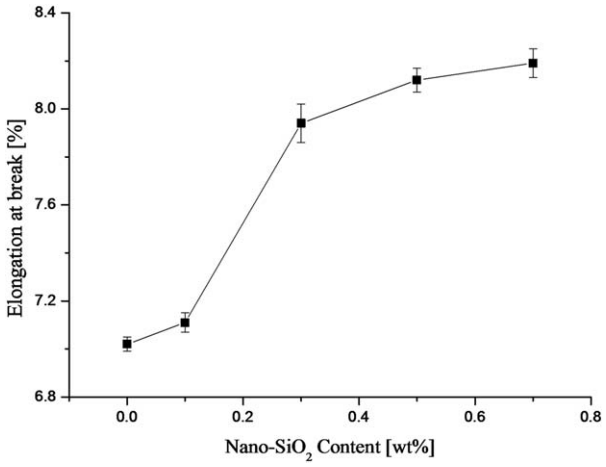

Figure 8. Elongation at break of the nanocomposites as a function of the nano-SiO_2 content.

Table III. Flexural Properties of the Unfilled Resin and Nanocomposites

Resin	E_f (GPa)	Σ_{max} (MPa)	E_{max} (%)
Unfilled resin	1.7 ± 0.03	31.6 ± 0.15	1.40 ± 0.04
3DP-1	6.7 ± 0.10	69.3 ± 0.20	1.74 ± 0.03
3DP-2	8.3 ± 0.06	108.5 ± 0.15	1.79 ± 0.06
3DP-3	7.9 ± 0.05	101.7 ± 0.09	2.14 ± 0.04
3DP-4	8.0 ± 0.05	90.5 ± 0.15	2.34 ± 0.04

E_f: flexural modulus; Σ_{max}: maximum flexural strength; E_{max}: maximum strain at break.

and the polymer resin was weak, and the load transfer from the polymer to the nano-SiO_2 was not large enough for the nano-SiO_2 to be broken under tensile loading. Instead, the nano-SiO_2 tended to be pulled out. The second reason was related to the structure of the outer shells of the nano-SiO_2. Because weak van der Waal's forces existed between individual graphene shells of the nano-SiO_2, slippage between the shells occurred.

Flexural Properties. To quantify the effect of the nano-SiO_2 component on the bending properties of nanocomposites, three-point flexural testing experiments were conducted. These composites showed the characteristics of quasi-brittle materials, all specimens fracturing at a strain close to the maximum in the flexural stress–strain curve. The results presented in Table III showed that the addition of 0.7 wt % nano-SiO_2 to the photocurable resin increased the flexural modulus from 1.7 to 8.0 GPa. The maximum flexural strength and strain at break increased from 31.6 MPa and 1.40%, respectively, to 108.5 MPa and 2.34%, which was explained by the same reason as the result of the tensile properties.

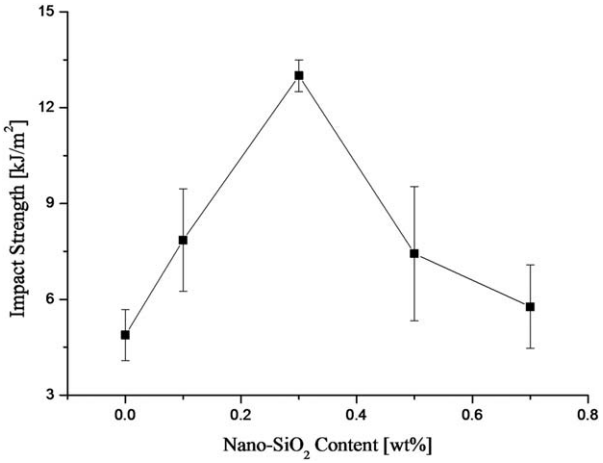

Figure 9. Impact strength of the unfilled resin and nanocomposites with different contents of nano-SiO_2.

Impact Properties. The role of the nano-SiO_2 content on the impact behavior of the nanocomposites is shown in Figure 9. A

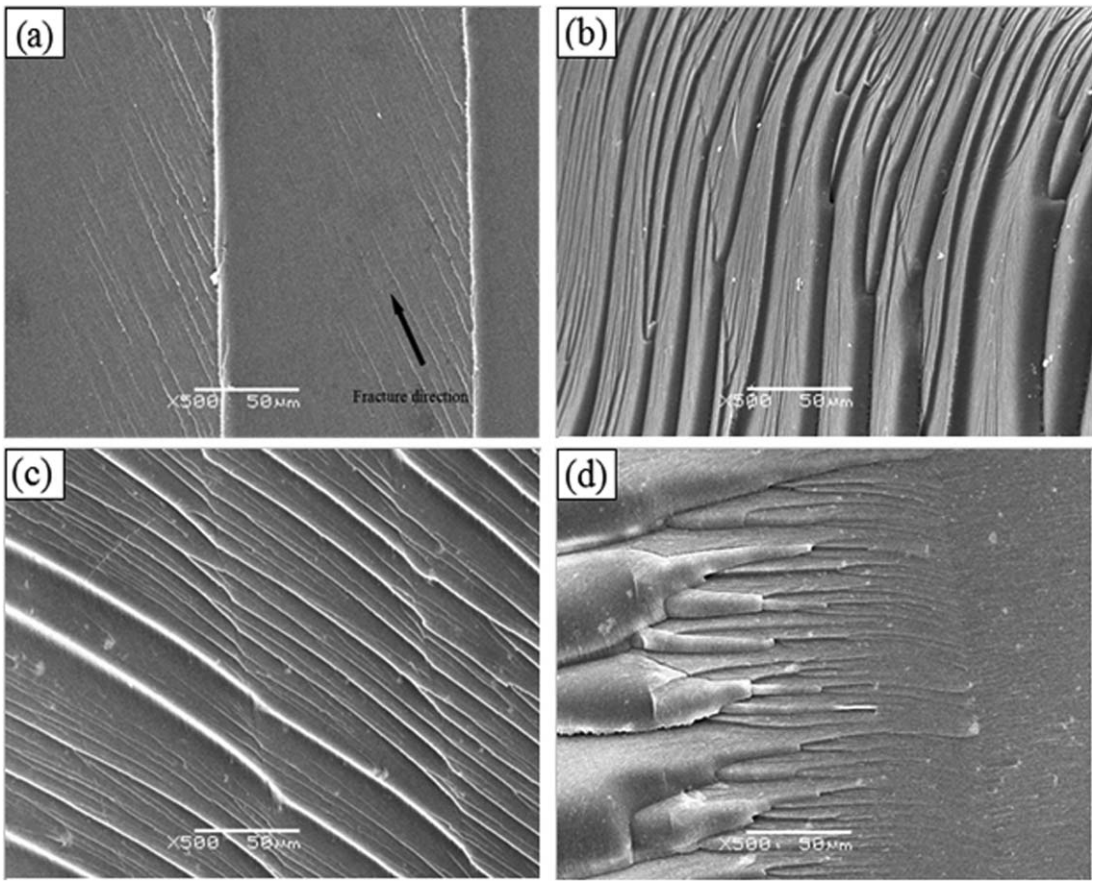

Figure 10. Fracture surfaces of the (a) unfilled resin, (b) 0.3 wt % nano-SiO_2, (c) 0.5 wt % nano-SiO_2, and (d) 0.7 wt % nano-SiO_2.

far more dramatic increase in the impact strength of 165.3% (from 4.9 to 13.0 kJ/m^2) was obtained with the addition of 0.3 wt % nano-SiO_2 to the photocurable resin. Figure 9 shows that the contribution of a low content of nano-SiO_2 changed the impact strength of the nanocomposite slightly. However, the nanocomposites with nano-SiO_2 contents higher than 0.3 wt % demonstrated considerable changes in the impact properties. This improvement was comparable to the toughening effect of polyurethane,[29] and nano-SiO_2 toughening was achieved at a lower filler content.

To investigate the toughening mechanisms, the fracture surfaces of the broken specimens after the impact tests were examined with scanning electron microscopy, as shown in Figure 10. It was obvious that the presence of nano-SiO_2 in the resins strongly influenced the surface morphology of the networks. The fracture surface is observable in Figure 10(a); this figure indicates a smooth surface with groove patterns. The groove pattern matched the direction of crack propagation; this is indicated by an arrow in Figure 10(a). Such features of the fracture surface represented the brittle behavior of the unfilled resin.

In stark contrast, the fracture surfaces of the nanocomposites blended with increasing amounts of nano-SiO_2 were relatively rougher and covered with particles. As shown by the micrograph in Figure 10(b), the nano-SiO_2 hindered the crack propagation by deflection, blocking, or crack bridging. The graphs in Figure 10(c,d) show that the nano-SiO_2 debonding phenomenon appeared seriously at the matrix, and this was harmful to the mechanical properties of the nanocomposites and was consistent with the experimental results. As mentioned previously, the nano-SiO_2 played an important role in stopping the running crack; this dissipated tremendous fracture energy and led to an enhancement in the impact resistance of the composites.

CONCLUSIONS

A systematic study was explored about how the introduction of small amounts of nano-SiO_2 (i.e., <1 wt %) affected the mechanical properties of UV-curing materials. The morphology, photochemistry, thermal properties, and mechanical properties of the nanocomposites were experimentally examined with the content of modified nano-SiO_2 being increased up to 0.7 wt %. The nanocomposites were readily accessible by a ball-milling technique. With an increasing minute amount of nano-SiO_2, the viscosities increased slightly, but the nanocomposites were still available for UV-curing 3DP processing:

1. FTIR spectroscopy and TEM showed an efficient surface-treatment approach of nano-SiO_2; this made a great contribution to the dispersion of nano-SiO_2 in the matrix and the combination of nano-SiO_2 with the polymer.
2. The investigation of photochemistry revealed that the increasing filler content led to a slightly decreased C_d for a given E, whereas E_c acted the opposite.
3. The addition of nano-SiO_2 increased the T_g values of the UV-curable nanocomposites. When the nano-SiO_2 content was 0.7 wt %, T_g reached the maximum value of 80.1°C; this was 12.9°C higher than that of the unfilled resin.
4. More improved tensile strengths and elongations at break were measured; these appeared to originate from the high level of dispersion and the intimate contact of nano-SiO_2 with the matrix and the impact strength. The scanning electron microscopy images of the fracture surface showed that typical ductile fracture occurred with increasing content of nano-SiO_2.

ACKNOWLEDGMENTS

This work was based on a project funded by Priority Academic Program Development of Jiangsu Higher Education Institutions and on a research and property evaluation system investigation of low-viscosity and environmentally friendly microspray 3DP materials. It was supported by Key Science and Technology Supporting Projects of Jiangsu Province (contract grant number BE2013012-3).

REFERENCES

1. Ingole, D. S.; Kuthe, A. M.; Thakare, A. M.; Talankar, A. S. *Rapid Prototyping J.* **2009**, *15*, 280.
2. Cesaretti, G.; Dini, E.; Kestelier, E.; Colla, V.; Pambaguian, L. *Acta Astronaut.* **2014**, *93*, 430.
3. Breuer, O.; Tchoudakov, R.; Narkis, M.; Siegmann, A. *J. Appl. Polym. Sci.* **1997**, *64*, 1097.
4. Berman, B. *Bus. Horiz.* **2012**, *55*, 155.
5. Lee, J. Y.; Choi, B.; Wu, B.; Lee, M. *Biofabrication* **2013**, *5*, 1.
6. Poodts, E.; Minak, E. *Rapid Prototyping J.* **2013**, *19*, 327.
7. Karalekas, D. E. *Mater. Des.* **2003**, *24*, 665.
8. Ferreira, J. C.; Santos, J. C.; Madureira, H.; Castro, H. *Rapid Prototyping J.* **2006**, *12*, 18.
9. Melchels, F. P. W.; Jan, F. J.; Grijpma, D. W. *Biomaterials* **2010**, *31*, 6121.
10. Das, D.; Satapathy, B. K. *Mater. Des.* **2014**, *54*, 712.
11. Salmi, M.; Paloheimo, K. S.; Tuomi, K. S.; Wolff, J.; Makitie, A. *J. Craniomaxillofac. Surg.* **2012**, *11*, 1.
12. Rahmanian, S.; Suraya, S.; Shazed, M. A.; Zahari, M. A.; Zainudin, E. S. *Mater. Des.* **2014**, *60*, 34.
13. Hsu, C. Y.; Huang, C. K.; Tzou, G. *J. Rapid Prototyping J.* **2008**, *14*, 102.
14. Almuhammadi, K.; Alfanoa, M.; Yang, Y.; Lubineau, G. *Mater. Des.* **2014**, *53*, 921.
15. Kumar, S.; Hofmann, S.; Steinmann, B.; Foster, E. J.; Weder, C. *ACS Appl. Mater. Interfaces* **2012**, *4*, 5399.
16. Cadek, M.; Coleman, M.; Ryan, K. P. *Nanoletters* **2004**, *4*, 353.
17. Gurr, M.; Hofmann, D.; Ehm, D.; Thomann, Y.; Kubler, Y.; lhaupt, R. M. *Adv. Funct. Mater.* **2008**, *18*, 2390.
18. Martone, A.; Formicola, C.; Giordano, M.; Zarrelli, M. *Compos. Sci. Technol.* **2010**, *70*, 1154.
19. Shazed, M. A.; Suraya, A. R.; Rahmanian, S.; Mohd Salleh, M. A. *Mater. Des.* **2014**, *54*, 660.

20. Liu, X. Q.; Yang, W.; Xie, B. H.; Yang, M. B. *Mater. Des.* **2012**, *34*, 355.
21. Bose, S.; Khare, R. A.; Moldenaers, P. *Polymer* **2010**, *51*, 975.
22. Cui, L. J.; Wang, Y. B.; Xiu, W. *J. Mater. Des.* **2013**, *49*, 279.
23. Yang, Z. H.; Ni, A. Q.; Wang, J. H. *J. Appl. Polym. Sci.* **2013**, *10*, 2905.
24. Zhou, Z.; Wang, S. F.; Lu, L.; Zhang, Y. X.; Zhang, Y. *Compos. Sci. Technol.* **2008**, *68*, 1727.
25. Mazov, I. N.; Ilinykh, I. N.; Kuznetsov, V. L. *J. Alloys Compd.* **2014**, *586*, 440.
26. Jacobs, P. F. *Soc. Manuf. Eng.* **1992**, *12*, 25.
27. Paul, J.; Romeis, J.; Mackovic, M. *Powder Technol.* **2015**, *27*, 337.
28. Song, Y.; Yu, J. H.; Dai, D.; Song, L. X.; Jiang, N. *Mater. Des.* **2014**, *64*, 687.
29. Chang, C. W.; Lu, C. W. *J. Appl. Polym. Sci.* **2010**, *115*, 2197.